Annals of Nuclear Energy 62 (2013) 564–571

Contents lists available at SciVerse ScienceDirect

Annals of Nuclear Energy

journal homepage: www.elsevier.com/locate/anucene

A highly accurate algorithm for the solution of the point kinetics equations

B.D. Ganapol *

Department of Aerospace and Mechanical Engineering, University of Arizona, RM 727, AME Bldg., Tucson, AZ 85721, United States

ARTICLE INFO

Article history:
Available online 9 January 2013

Keywords:
Point kinetics equations
Backward Euler finite difference
Romberg acceleration
Convergence acceleration

ABSTRACT

Attempts to resolve the point kinetics equations (PKEs) describing nuclear reactor transients have been the subject of numerous articles and texts over the past 50 years. Some very innovative methods, such as the RTS (Reactor Transient Simulation) and CAC (Continuous Analytical Continuation) methods of G.R. Keepin and J. Vigil respectively, have been shown to be exceptionally useful. Recently however, several authors have developed methods they consider accurate without a clear basis for their assertion. In response, this presentation will establish a definitive set of benchmarks to enable those developing PKE methods to truthfully assess the degree of accuracy of their methods. Then, with these benchmarks, two recently published methods, found in this journal will be shown to be less accurate than claimed and a legacy method from 1984 will be confirmed.

1. My concern

The solution to the point kinetics equations, central to nuclear reactor transient analysis, is a challenge that has yet to be satisfactory resolved. There have been several notable historic attempts including those of Nobrega (1971), Keepin (1965), Vigil (1967), Izumi and Noda (1971) and others who, in effect, have provided only modest improvements (if any) over these original methods. In several recent publications however, we find authors presenting numerical schemes with little or no change from those presented earlier. In addition, they have made claims of accuracy that are not based on true benchmarks, but on ad hoc comparisons to other methods. We find numerical values, published to four, five or more places of inferred accuracy, when indeed this is not the case. These articles go under the titles of an *efficient technique* (Nahla, 2011; Aboanber and Hamada, 2002, 2003), *analytical solution* (Nahla, 2010; Petersen et al., 2011), *analytical exponential method* (Nahla, 2008) and *analytical inversion method* (Aboanber and Nahla, 2002). In reality, none of the methods listed are either analytical or truly efficient or, more importantly, of benchmark accuracy defined here to be a consistent 5–9 places.

As an example, we focus on an article entitled "An efficient technique for the point kinetics equations with Newtonian temperature feedback effects" (Nahla, 2011). In this work, we find an ad hoc separation of the non-linear reactivity identical to that found in (Kinard and Allen, 2004). There follows a finite difference development that uses an implicit backward Euler (BE) finite difference (FD) scheme to give an explicit extrapolated value of the unknown (non-linear) reactivity at the next time interval. We then return to the analytical form of the original equation with the (known) advanced reactivity inserted and to be solved analytically, over a time step, as a set of 7 ODEs now with constant reactivity. In the process, there is a rather unorthodox solution to the inhour equation that seems overly complicated and entirely unnecessary, given that one is simply solving for the zeros of a polynomial. The author then compares his results with standard step input and ramp results quoting 5 digits that are in excellent agreement with the literature. Of particular note, the method is tested only for power transients of less than 32 times nominal and not for severe transients. Finally, there is no self-consistency check reported to ensure internal accuracy. Thus, the method has not been thoroughly verified leaving open the question of its overall performance, especially for severe transients. In the final section of the aforementioned article, there are several tables of neutron densities for the case with temperature feedback. The entries are compared to several other methods, where no two methods agree to more than two places while the author quotes 7 digits (6 places). Clearly, any conclusion regarding the merit of the "efficient technique" has no basis without further evidence. In spite of this, the author concludes.

> *"These comparisons substantiated the accuracy, faster [speed] and the efficiency of the efficient techniques."*

The investigation to follow demonstrates that benchmark accuracy of 9-places or more can come from the same basic BEFD scheme found in (Nahla, 2011). Not only, will the simple BE approximation be used in a most efficient way, but also there will be no need to solve the inhour equation, greatly simplifying the

* Tel.: +1 520 621 4728; fax: +1 520 621 8191.
E-mail address: ganapol@cowboy.ame.arizona.edu

0306-4549/$ - see front matter © 2012 Elsevier Ltd. All rights reserved.
http://dx.doi.org/10.1016/j.anucene.2012.06.007

overall numerical evaluation. In addition, definitive benchmarks will be established for use as standards to enable truthful statements concerning the accuracy of new methods. It must also be remarked, that, arguably, with establishment of the PKE/BEFD algorithm to be presented, there may be no need for future numerical algorithms to solve the PKEs.

2. The backward Euler finite difference (BEFD) approximation

We begin with the point kinetics equations with feedback for m delayed neutron groups

$$\begin{aligned}\frac{dN(t)}{dt} &= \left[\frac{\rho(t,N)-\beta}{\Lambda}\right]N(t)+\sum_{l=1}^{m}\lambda_l C_l(t)+q(t)\\ \frac{dC_l(t)}{dt} &= \frac{\beta_l}{\Lambda}N(t)-\lambda_l C_l(t),\quad l=1,\ldots,m\end{aligned} \tag{1a}$$

and generally including Newtonian feedback

$$\rho(t,N)=\rho_0(t)-B\int_0^t dt' N(t') \tag{1b}$$

as our initial consideration.

All the symbols have their usual meanings (N is power or neutron density, C_l is the precursor concentration in group l, ρ is reactivity, q is an external source, β_l is the yield from fission of precursors in delayed group l and β is the total yield, λ_l is the precursor decay constant for group l, Λ is the neutron generation time, B is the absolute value of the temperature coefficient of reactivity and ρ_0 is a prescribed reactivity). Note that Eq. (1b) can also be written as

$$\frac{d\rho(t,N)}{dt}=\frac{d\rho_0(t)}{dt}-BN(t) \tag{2}$$

leading to the more condensed vector form for Eqs. (1) and (2)

$$\frac{d\mathbf{y}(t)}{dt}=\mathbf{A}(t,N(t))\mathbf{y}(t)+\mathbf{q}(t) \tag{3a}$$

with

$$\mathbf{y}(t)\equiv\begin{bmatrix}N(t)\\ C_1(t)\\ \cdots\\ C_l(t)\\ \rho(t)\end{bmatrix},\quad \mathbf{q}(t)\equiv\begin{bmatrix}q(t)\\ 0\\ \cdots\\ 0\\ \dfrac{d\rho_0}{dt}\end{bmatrix} \tag{3b}$$

The Jacobian matrix is

$$\mathbf{A}(t,N(t))\equiv\begin{bmatrix}(\rho(t,N(t))-\beta)/\Lambda & \lambda_1 & \lambda_2 & \cdots & \lambda_m & 0\\ \frac{\beta_1}{\Lambda} & -\lambda_1 & 0 & \cdots & \cdots & 0\\ \frac{\beta_2}{\Lambda} & 0 & -\lambda_2 & & & \cdots\\ \cdots & \cdots & & \cdots & & \cdots\\ \frac{\beta_m}{\Lambda} & 0 & \cdots & 0 & -\lambda_m & 0\\ -B & 0 & \cdots & & \cdots & 0\end{bmatrix} \tag{3c}$$

and Eq. (3a) is to be solved subject to the following initial conditions:

$$\mathbf{y}(0)\equiv\begin{bmatrix}N(0)\\ \frac{\beta_1}{\lambda_1\Lambda}N(0)\\ \cdots\\ \frac{\beta_m}{\lambda_m\Lambda}N(0)\\ \rho_0(0)\end{bmatrix} \tag{3d}$$

A straightforward derivation of the BEFD approximation begins with the following Taylor series (from above in time) at time t_j ($h=t_{j+1}-t_j$):

$$\mathbf{y}(t_j)=\mathbf{y}(t_{j+1})-h\left.\frac{d\mathbf{y}(t)}{dt}\right|_{t_{j+1}}+\sum_{k=2}^{\infty}\frac{(-1)^k}{k!}\mathbf{y}^{(k)}(t_{j+1})h^k \tag{4}$$

to also play a primary role below. With substitution of Eqs. (3a) and (4) becomes

$$\begin{aligned}\mathbf{y}(t_j)=\mathbf{y}(t_{j+1})&-h[\mathbf{A}(t_{j+1},N(t_{j+1}))\mathbf{y}(t_{j+1})+\mathbf{q}(t_{j+1})]\\ &+\sum_{k=2}^{\infty}\frac{(-1)^k}{k!}\mathbf{y}^{(k)}(t_{j+1})h^k\end{aligned}$$

The implicit BEFD approximation is then the first three terms of this equation

$$[\mathbf{I}-h\mathbf{A}(t_{j+1},N(t_{j+1}))]\mathbf{y}_{j+1}=\mathbf{y}_j+h\mathbf{q}(t_{j+1})$$

or, on inversion

$$\mathbf{y}_{j+1}=[\mathbf{I}-h\mathbf{A}(t_{j+1},\tilde{N})]^{-1}[\mathbf{y}_j+h\mathbf{q}(t_{j+1})] \tag{5}$$

Note when t_j is in an argument, then the quantity is considered to be exact and to be approximated by the same variable when subscripted.

At this point, we assume that the neutron density $[\tilde{N}]$ in the Jacobian matrix $\mathbf{A}$ is known and represents a first approximation to the fixed-point iteration to be described. As shown by Nobrega (Nobrega, 1971), the sparse $\mathbf{A}$-matrix conveniently lends itself to the analytical inversion

$$[\mathbf{I}-h\mathbf{A}]^{-1}\equiv\frac{1}{\sigma}\begin{bmatrix}1\\ \frac{h\beta_1/\Lambda}{1+h\lambda_1}\\ \cdots\\ \frac{h\beta_m/\Lambda}{1+h\lambda_m}\\ -hB\end{bmatrix}\begin{bmatrix}1\\ \frac{h\lambda_1}{1+h\lambda_1}\\ \cdots\\ \frac{h\lambda_m}{1+h\lambda_m}\\ 0\end{bmatrix}^T+\begin{bmatrix}0 & 0 & \cdots & & 0\\ 0 & \frac{1}{1+h\lambda_1} & & & \\ \cdots & & \cdots & & \\ & & & \frac{1}{1+h\lambda_m} & 0\\ 0 & & & 0 & 1\end{bmatrix}$$

with

$$\sigma\equiv 1-h\frac{\rho(t_{j+1},\tilde{N})}{\Lambda}+\sum_{l=1}^{m}\frac{h\beta_l/\Lambda}{1+h\lambda_l}.$$

When σ is zero the last expression becomes the inhour equation. We now focus on the numerical algorithm to solve Eq. (5).

3. The PKE/BEFD algorithm and its implementation

The error of the BE approximation can be found by noting that the true solution and approximate solutions are formally related by

$$\mathbf{y}(t_{j+1})=\mathbf{y}_{j+1}+\boldsymbol{\varepsilon}_{j+1} \tag{6}$$

By expansion of the inverse in small h in the approximate solution to Eq. (5) formally satisfies

$$\mathbf{y}_{j+1}=\mathbf{y}_j+\sum_{k=1}^{\infty}\boldsymbol{\beta}_{kj}h^k \tag{7a}$$

and from Eq. (4)

$$\mathbf{y}(t_{j+1})=\mathbf{y}(t_j)+\sum_{k=1}^{\infty}\boldsymbol{\gamma}_{kj}h^k. \tag{7b}$$

Subtracting Eqs. (7a) from (7b) and noting Eq. (6) gives

$$\boldsymbol{\varepsilon}_{j+1}=\boldsymbol{\varepsilon}_j+\sum_{k=1}^{\infty}[\boldsymbol{\gamma}_{kj}-\boldsymbol{\beta}_{kj}]h^k \tag{8}$$

Then, on summing over j on $[0, j]$, one finds an explicit form of the error

$$\boldsymbol{\varepsilon}_{j+1} = \sum_{k=1}^{\infty}\left\{\sum_{j'=0}^{j}[\boldsymbol{\gamma}_{kj'} - \boldsymbol{\beta}_{kj'}]\right\}h^k = \sum_{k=1}^{\infty}\mathbf{c}_{kj}h^k \tag{9}$$

that will allow a consistent extrapolation to give higher order approximations to the original BEFD approximation. The extrapolation is essentially a copy of the evaluation of an integral by Romberg integration called Richardsons extrapolation. The initial (zeroth) approximation is Eq. (5), which from Eqs. (6) and (9) gives for the true solution at t_{j+1}

$$\mathbf{y}(t_{j+1}) = \mathbf{y}_{j+1}(h) + \sum_{k=1}^{\infty}\mathbf{c}_{kj}h^k. \tag{10}$$

Calling the zeroth approximation at t_{j+1}

$$\boldsymbol{\phi}_0(h) = \mathbf{y}_{j+1}(h) \tag{11a}$$

and continuing to eliminate higher orders in h gives Richardsons deferred approach to the limit (Stoer, 1980)

$$\boldsymbol{\phi}_s(h) = \frac{2^s\boldsymbol{\phi}_{s-1}(h/2) - \boldsymbol{\phi}_{s-1}(h)}{2^s - 1} \tag{11b}$$

and the exact solution is therefore approximated to order h^{s+1} as

$$\mathbf{y}(t_{j+1}) = \boldsymbol{\phi}_s(h) + O(h^{s+1}) \tag{11c}$$

The elimination continues numerically until the relative error of two extrapolations is within a desired tolerance.

The implementation simply requires the specification of edits defining original edit intervals, which are sequentially partitioned by two to give a sequence of approximations $\phi_s(h)$ (one approximation for each grid s) for **y** at the end of the interval. The Richardsons converged approximation [from Eq. (11b)] then provides the initial condition for the next original edit interval. Having a highly accurate initial condition at the start of an interval greatly reduces propagation error accumulation—the primary source of error in an initial value problem. To further reduce the error, if any density values are negative in any grid, that grid is ignored by continuing on to the next one. If convergence is not achieved by the end of, say 14 subdivisions (2^{14} sub-edits), the original edit interval is subdivided by 2 and the procedure begins anew for the subdivided original edit intervals. The entire procedure can be further accelerated by subdividing the original edit intervals into sub-original intervals (requiring more edits) at the start the calculation.

4. Some numerical comparisons

In this section, we take a critical look at the all results of (Nahla, 2011) and some from (Aboanber and Hamada, 2003). This demonstration features step, ramp and sinusoidal reactivity insertions as well as non-linear temperature feedback.

4.1. Prescribed insertions (B = 0)

For the following examples, with the temperature coefficient B of zero, the reactivity is considered known and therefore removed from the vector **y** reducing the order of **A**.

4.1.1. Step insertion

The first example is for step insertion. Actually, once the eigenvalues of the ***A***-matrix are known, the solution for this case is analytically expressed as a sum of exponentials through linear algebra considerations. Thus, a numerical solution is not truly required for this case other than for the solution to the inhour equation.

Table 1b gives the neutron density for the thermal reactor I whose kinetic parameters are given in Table 1a. Nine correct places provide extraordinary accuracy. In addition, $t = 100s$ is included for all reactivities to give a more challenging benchmark. One expects all values to be accurate to one digit in the last place.

Table 1a
Thermal reactor I with $\Lambda = 5 \times 10^{-4}$ s.

l	β_l	λ_l (s^{-1})
1	0.000285	0.0127
2	0.0015975	0.0317
3	0.001410	0.115
4	0.0030525	0.311
5	0.00096	1.40
6	0.000195	3.87
	$\beta = 0.0075$	

Table 1b
Neutron density for step insertions.

$t(s)/\rho(\$)$	−1	−0.5	0.5
1.0000E−01	5.205642866E−01	6.989252256E−01	1.533112646E+00
1.0000E+00	4.33333**4**453E−01	6.070535656E−01	2.511494291E+00
1.0000E+01	2.361106508E−01	3.960776907E−01	1.421502524E+01
1.0000E+02	2.866764245E−02	7.158285444E−02	8.006143562E+07
$t/\rho(\$)$			1
1.0000E−01			2.515766141E+00
5.0000E−01			1.036253381E+01
1.0000E+00			3.218354095E+01
1.0000E+01			3.246978898E+09
1.0000E+02			2.596484646E+89

Table 1c
Neutron density for step insertions $\rho = \$1$.

t(s)	BEFD	Exact
1.00E−01	2.5157661414043723001E+00	2.5157661414043723001E+00
5.00E−01	1.0362533810640214680E+01	1.0362533810640214680E+01
1.00E+00	3.2183540945534212174E+01	3.2183540945534212174E+01
1.00E+01	3.2469788980305281367E+09	3.2469788980305281366E+09
1.00E+02	2.5964846465508730749E+89	2.5964846465508730749E+89

When rounded, except for the one emboldened digit, PKE/BEFD values are identical to the exact values in Table 1 of (Nahla, 2011). The discrepancy is most likely a rounding error.

To assess the advantage of the Richardsons acceleration, Fig. 1 shows the relative error without acceleration. The accumulation of propagation error with increasing time is quite apparent.

Table 1c is included to show that all is not perfect with the BEFD scheme. Run in quadruple precision, the table presents the neutron density to 19 places for both the exact calculation using basic

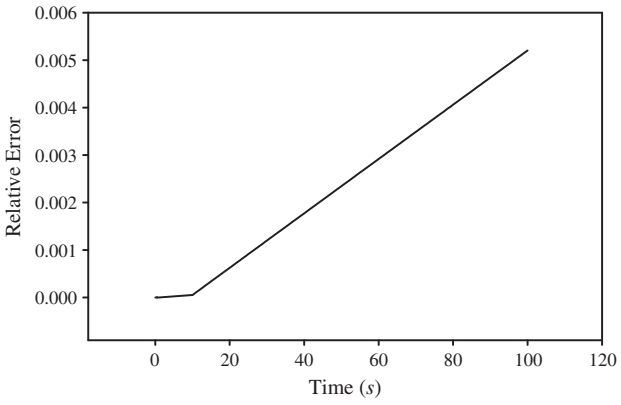

Fig. 1. Step insertion without acceleration.

Table 2a
Thermal reactor II with $\Lambda = 2 \times 10^{-5}$ s.

l	β_l	$\lambda_l(s^{-1})$
1	0.000266	0.0127
2	0.001491	0.0317
3	0.001316	0.115
4	0.002849	0.311
5	0.000896	1.40
6	0.000182	3.87
	$\beta = 0.007$	

Table 2b
Neutron density for ramp insertion of 0.1 \$/s.

t(s)	N
2.0000E+00	1.338200050E+00
4.0000E+00	2.228441897E+00
6.0000E+00	5.582**0**52449E+00
8.0000E+00	4.278629573E+01
1.0000E+01	4.511636239E+05
1.1000E+01	1.792213607E+16

matrix algebra and the BEFD scheme. Note that the 19th digit of the BEFD calculation for $t = 10s$ is off by one unit.

4.1.2. Ramp insertion

The second comparison is for a ramp insertion of $0.1\$/s$ for thermal reactor II with kinetic parameters given in Table 2a. The PKE/BEFD values are given in Table 2b.

Again, when rounded, all five digits, except for the one emboldened digit, agree with the results of the efficient technique of (Nahla, 2011) shown in Table 2 of that reference. The general superiority of the PKE/BEFD and the efficient technique with respect to four of the six comparison methods surveyed in (Nahla, 2011) is evident (i.e., not all digits agree to the BEFD benchmark). This however is not to imply that the efficient technique can reproduce all 9 digits, which is highly doubtful. A more demanding value of density at $t = 11s$ is included to give a more meaningful test set.

4.1.3. Sinusoidal insertion

The final prescribed reactivity is for one delayed group in a fast reactor with $\beta = 0.0079$ and $\lambda = 0.077$/s and a sinusoidal reactivity $\rho(t) = \rho_0 \sin(\pi t/T)$. The neutron generation time is $\Lambda = 10^{-8}$ s.

Two benchmarks will be given here. The first is for the neutron density, given in Table 3a for $\rho_0 = 0.0053333$ and $T = 50s$. These values were not provided by Nahla (2011), but are of diagnostic value nevertheless. A plot of the density is shown in Fig. 2a for one full cycle and for 10 cycles in Fig. 2b. Achieving stability for the latter case should be a challenge for any numerical method.

The second benchmark is designed to accurately determine (to 6-places) the time to the first peak and the peak neutron density for the four sinusoidal insertions given in Table 3b. This is most easily done by interrogating the derivative of N from Eq. (3a) and capturing the sign changes until the time between changes becomes acceptably small –which here will be to a relative error of 10^{-7}. The time to the peak and the peak values are also found in Table 3b. The emboldened digits are from Table 3 of the "efficient technique" (Nahla, 2011) and are in disagreement with the BEFD results. It should be emphasized that Table 3b gives the first true benchmark for peak times and neutron densities for a sinusoidal reactivity—a case of interest for nearly 40 years.

Fig. 2c shows the variation over $1000s$ for all four cases—again a challenge for a numerical method to duplicate.

Table 3a
Neutron Densities for sinusoidal reactivity variation $\rho_0 = 0.0053333$, $T = 50$ s.

t(s)	N
10.0	2.065383519E+00
20.0	8.854133921E+00
30.0	4.064354222E+01
40.0	6.135607517E+01
50.0	4.610628770E+01
60.0	2.912634840E+01
70.0	1.895177042E+01
80.0	1.393829211E+01
90.0	1.253353406E+01
100.0	1.544816514E+01

Table 3b
Times to first peak and peak densities.

$T(s)$	$\rho_0 \times 10^3$	$t_p(s)$	N_p	$t_p(s)$ [5, Table 3]	N_p[5, Table 3]
50	5.3333	3.910712E+01	6.153015E+01	3.91**11**E+01	6.153**1**E+01
150	3.2327	1.373198E+02	9.581150E+01	1.3732E+02	9.581**1**E+01
250	2.3193	2.371265E+02	1.134679E+02	2.371**2**E+02	1.134**6**E+02
350	1.8083	3.370713E+02	1.238209E+02	3.3707E+02	1.2382E+02

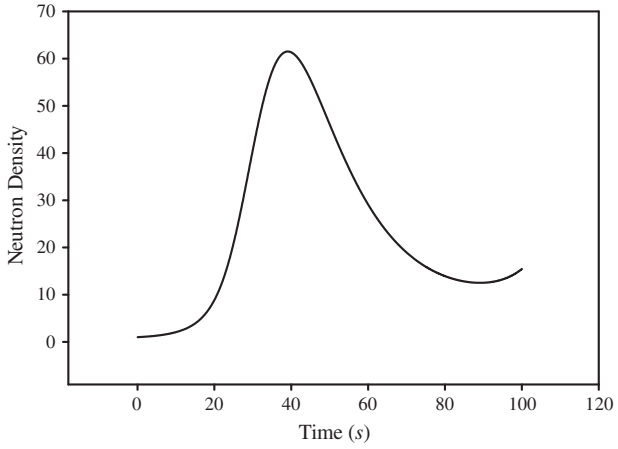

Fig. 2a. Neutron density variation for one cycle of a sinusoidal reactivity insertion.

4.2. Step insertion with temperature feedback

Finally, we come to the main theme of this analysis—non-linear temperature feedback– which shows the power of the PKE/BEFD solution. Now, the reactivity is a function of the neutron density N and iteration must be applied to achieve high accuracy.

Essentially, a fixed-point iteration is performed during each time step so the Eq. (5) reads

$$\mathbf{y}_{j+1}^{k+1} = [\mathbf{I} - h\mathbf{A}(t_{j+1}, N^k)]^{-1}[\mathbf{y}_j + h\mathbf{q}(t_{j+1})] \tag{12}$$

where N^k is updated until convergence. On convergence, $\mathbf{y}_{j+1}^{k+1}$ becomes the initial condition for the next interval. For the examples to follow, no more than 14 iterations on a grid were required for convergence to a relative accuracy of 10^{-10}.

4.2.1. Step insertion with temperature feedback

Table 4a gives a comparison of PKE/BE and the "efficient technique" (Nahla, 2011) for the thermal reactor III with kinetic parameters of Table 4b and for $B = 2.5 \times 10^{-6}$. Here, one can observe the poor performance of the efficient technique, even for step insertion. Of the 7-digits published for neutron density, agreement in

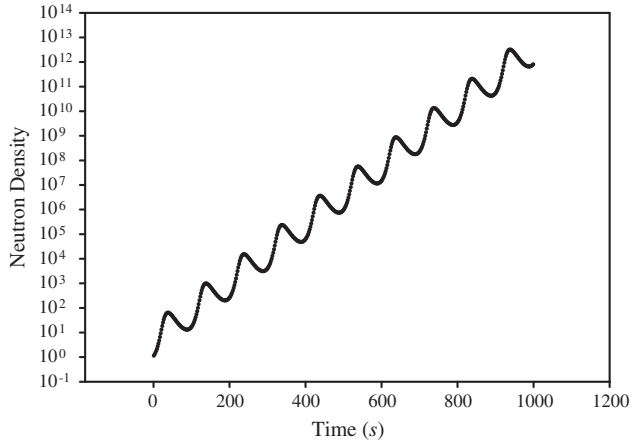

Fig. 2b. Neutron density variation for 10 cycles of a sinusoidal reactivity insertion.

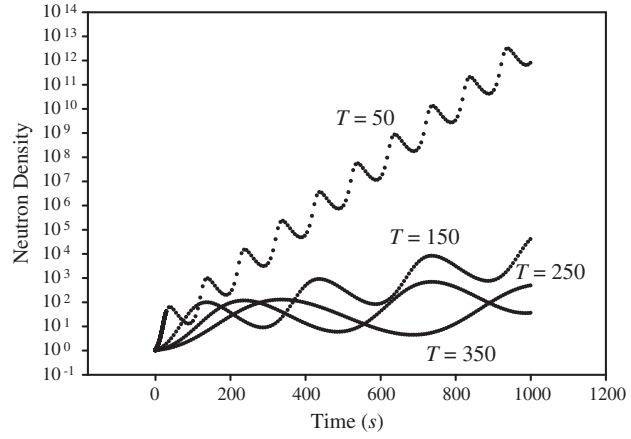

Fig. 2c. Neutron density variation for all four cases of sinusoidal reactivity insertion.

a few cases is to only 3 or 4-digits at best; otherwise, only 2-digit agreement is found. It should be noted that nearly consistent 4-digit agreement (except for the last case) is found for the "New Analytic Method (NAM)" (Nahla, 2010) whose results are also quoted in (Nahla, 2011).

Hence, the accuracy of the "efficient technique" is far from "substantiated" as claimed and publishing 7-digit results is certainly unnecessary.

To complete this example, Fig. 3 displays the neutron density trace for several step reactivity insertions with feedback. The delay in the time when the feedback kicks in is clearly apparent.

It is a relatively simple matter to determine the time to peak t_p and the peak neutron density N_p as in the previous example. Of the seven digits reported in Table 4c for the peak density, the best agreement in (Nahla, 2011) is to 4 digits at ρ_0 = \$0.5 and the worst is one at ρ_0 = \$2.0. For the time to peak density, there is agreement to only two or three places. As before, the claims of accuracy are greatly exaggerated. Curiously, again there is 4-or 5-digit agreement with the NAM method Nahla, 2010).

4.2.2. Ramp insertion with temperature feedback

Now, we consider the comprehensive feedback example of compensated reactor shutdown (Keepin, 1965) as shown in Fig. 4 using the data of Table 4b. This is a classic example of transient initiation by ramp with ramp rate a and strong Doppler shutdown.

Table 4a
Neutron Density with feedback for $B = 2.5 \times 10^{-6}$.

ρ = \$1	t (s)	N	N[5, Table 5]
	1.000000000E+01	1.320385964E+02	1.321052E+02
	2.000000000E+01	5.169986095E+01	5.172712E+01
	3.000000000E+01	2.817468536E+01	2.818947E+01
	4.000000000E+01	1.814633000E+01	1.815454E+01
	5.000000000E+01	1.277957703E+01	1.278886E+01
	6.000000000E+01	9.474932501E+00	9.482830E+00
	7.000000000E+01	7.244477494E+00	7.248503E+00
	8.000000000E+01	5.646289700E+00	5.646767E+00
	9.000000000E+01	4.456834255E+00	4.458845E+00
	1.000000000E+02	3.550102766E+00	3.550773E+00
ρ = \$1.5			N[5, Table 6)]
	1.000000000E+01	1.079116832E+02	1.085460E+02
	2.000000000E+01	4.160428128E+01	4.183258E+01
	3.000000000E+01	2.329893150E+01	2.341236E+01
	4.000000000E+01	1.530342749E+01	1.536867E+01
	5.000000000E+01	1.089014315E+01	1.093202E+01
	6.000000000E+01	8.101031859E+00	8.130170E+00
	7.000000000E+01	6.182690459E+00	6.204616E+00
	8.000000000E+01	4.793307820E+00	4.812251E+00
	9.000000000E+01	3.755614629E+00	3.769579E+00
	1.000000000E+02	2.966074952E+00	2.965561E+00
ρ = \$2			N[5, Table 7)]
	1.000000000E+01	1.033808535E+02	1.051118E+02
	2.000000000E+01	3.913886903E+01	3.977467E+01
	3.000000000E+01	2.200377721E+01	2.233538E+01
	4.000000000E+01	1.449367193E+01	1.469613E+01
	5.000000000E+01	1.031861108E+01	1.045320E+01
	6.000000000E+01	7.663319203E+00	7.761803E+00
	7.000000000E+01	5.829395378E+00	5.904826E+00
	8.000000000E+01	4.499427073E+00	4.559800E+00
	9.000000000E+01	3.507422663E+00	3.555554E+00
	1.000000000E+02	2.755126886E+00	2.795546E+00

Table 4b
Thermal reactor III with $\Lambda = 5 \times 10^{-5}$ s.

l	β_l	$\lambda_l(s^{-1})$
1	0.00021	0.0124
2	0.00141	0.0305
3	0.00127	0.111
4	0.00255	0.301
5	0.00074	1.13
6	0.00027	3.00
	β = 0.00645	

Table 4c
Times to first peak and peak density with feedback.

ρ_0(\$)	$t_p(s)$	N_p	$t_p(s)$ [5, Table 4]	N_p[5, Table 4]
1.0E−01	1.089694E+02	2.110490E+00	–	–
2.0E−01	9.236818E+01	5.699818E+00	–	–
5.0E−01	2.829469E+01	4.575243E+01	2.83**53**E+01	4.575**945**E+01
1.0E+00	9.534776E−01	8.078681E+02	9.5**5**E−01	8.0**51905**E+02
1.2E+00	3.165970E−01	8.021025E+03	–	–
1.5E+00	1.682894E−01	4.302461E+04	1.68E−01	4.**118377**E+04
2.0E+00	9.839055E−02	1.678457E+05	9.8E−02	1.**537353**E+05

We report the time to peak power and the peak power in comparison to (Aboanber and Hamada, 2003) in Table 5. This case is widely used as a benchmark in the literature, but until now, there were no definitively determined times to the first density peak. For the first time, Table 5 presents 7-place accurate times and powers to the first peak. In comparison to the results of (Aboanber and Hamada, 2003), there is essentially three-figure agreement (non-emboldened digits in the last two columns) in peak times and

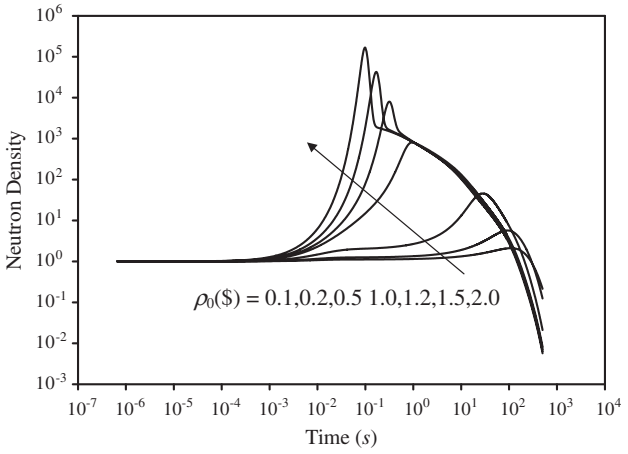

Fig. 3. Neutron density trace for step insertion with feedback.

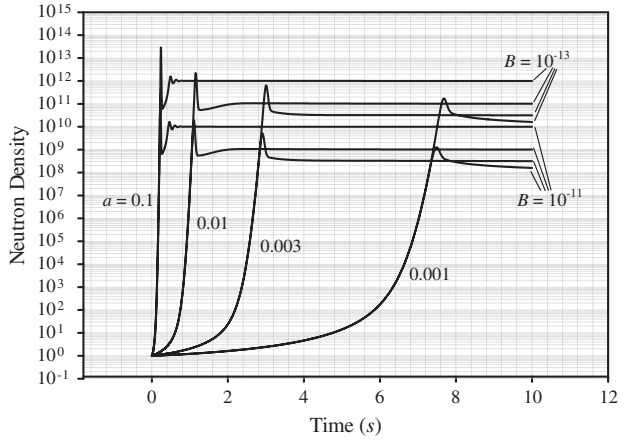

Fig. 4. Compensated reactor shutdown initiated by ramp.

Table 5
Time to peak and peak neutron density for ramp initiated adiabatic compensation with Doppler.

a (s^{-1})	B (cm^3/s)	t_{peak} (s)	N_{peak}	t_{peak} (s) [12, Table 4]	N_{peak} [12, Table 4]
0.1	10^{-11}	2.2466344E−01	2.4203815E+11	2.247**032**E−01	2.**395759**E+11
	10^{-13}	2.3890693E−01	2.8986741E+13	2.389**035**E−01	2.8**66668**E+13
0.01	10^{-11}	1.1060774E+00	2.0123519E+10	1.106**171**E+00	2.00**6490**E+10
	10^{-13}	1.1551476E+00	2.4911782E+12	1.155**279**E+00	2.4**83192**E+12
0.003	10^{-11}	2.9105821E+00	5.1141599E+09	2.91**0484**E+00	5.10**5933**E+09
	10^{-13}	3.0076015E+00	6.5344738E+11	3.00**7484**E+00	6.5**22229**E+11
0.001	10^{-11}	7.4887663E+00	1.2740752E+09	7.488**640**E+00	1.26**5265**E+09
	10^{-13}	7.6835876E+00	1.7210080E+11	7.6836**26**E+00	1.7**06856**E+11

barely two-place agreement in powers. Again, the relatively poor agreement for the number of digits reported hardly warrants a statement claiming method superiority (Aboanber and Hamada, 2003).

4.2.3. Simple kinetics and thermal hydraulics

The final example confirms an old kinetics solution methodology from 1984 and demonstrates the flexibility and versatility of the BEFD scheme. The method, called SKINATH (Dodds and Westfall, 1984) — Simple Kinetics and Thermal Hydraulics) —developed

Table 6a
Thermal reactor IV with $\Lambda = 5 \times 10^{-5}$ s.

l	β_l	λ_l (s^{-1})
1	0.00022	0.0124
2	0.00142	0.0305
3	0.00127	0.111
4	0.00257	0.301
5	0.00075	1.14
6	0.00027	3.01
	$\beta = 0.0065$	

Table 6b
BEFD.

t(min)	$N(t)$	$\rho(t)$	$T(t)$
0.000000000E+00	1.000000000E−02	4.300000000E+00	2.000000000E+01
1.000000000E+00	1.390664400E−02	4.299982607E−02	2.000005684E+01
1.000000000E+01	1.033074569E−01	4.299416065E−02	2.000190828E+01
1.000000000E+02	7.946137382E−01	−2.949530409E−02	4.369127585E+01
2.500000000E+02	2.118680532E−03	6.388467468E−03	3.196455312E+01
5.000000000E+02	9.818854372E−01	−4.825173107E−03	3.562914154E+01
7.500000000E+02	4.033472004E+00	−1.857286712E−03	3.465924402E+01
1.000000000E+03	7.680950791E+00	1.379148486E−03	3.360158546E+01
1.500000000E+03	1.502421669E+01	4.962590743E−04	3.389011141E+01
2.000000000E+03	1.358851928E+01	−2.104995975E−04	3.412107830E+01
2.500000000E+03	1.348250322E+01	3.094249800E−05	3.404217565E+01
3.000000000E+03	1.359755709E+01	3.819718029E−06	3.405103931E+01
4.000000000E+03	1.357214030E+01	5.947391521E−07	3.405209322E+01
SKINATH			
0.000000000E+00	1.000E−02	4.300E+00	2.000E+01
1.000000000E+00	1.391E−02	4.230E−02	2.000E+01
1.000000000E+01	1.033E−01	4.299E−02	2.000E+01
1.000000000E+02	7.946E−01	−2.950E−02	4.369E+01
2.500000000E+02	2.11**8**E−03	6.388E−03	3.196E+01
5.000000000E+02	9.819E−01	−4.82**6**E−03	3.563E+01
7.500000000E+02	4.033E+00	−1.85**8**E−03	3.466E+01
1.000000000E+03	7.68**0**E+00	1.379E−03	3.360E+01

for the IBM 3033 features double precision arithmetic. The numerical solution originates from the LSODE ordinary differential equation solver (Hindmarsh, 1980). The SKINATH code is applied to an air-cooled homogeneous cylindrical critical system for investigation of low power criticality accidents.

A simple thermal hydraulic model adds the following overall energy balance in terms of an average temperature

$$\frac{dT(t)}{dt} = \frac{1}{C_p}\left\{N(t) - ahd^{0.75}\left[1 - \frac{T_c}{T(t)}\right]^{0.25}[T(t) - T_c]\right\} \tag{13}$$

to Eqs. (1a). Here, C_p [$\sim 1.301 \times 10^4$ *Erg*/°C] is the system heat capacity, h and d are the system height and diameter, 23 cm, 20 cm, respectively, T_c is the initial temperature of 20 °C and a is a physical constant for air at STP and is 17.52. The reactivity is given by

$$\rho(t) = \rho_0 + \beta_T[T(t) - T_c] \tag{14}$$

where the assumed temperature coefficient of reactivity and initial reactivity are

$$\beta_T = -0.306\ ¢/°C$$
$$\rho_0 = 0.043\ ¢$$

Note that N is in units of power with an assumed initial value of $0.01W$.

A more convenient form for Eqs. (13) and (14) is

$$\frac{dW(t)}{dt} = \frac{1}{C_p}\left\{N(t) - ahd^{0.75}\left[\frac{W(t)}{W(t) + T_c}\right]^{0.25} W(t)\right\} \tag{15a}$$

$$\rho(t) = \rho_0 + \beta_T W(t) \tag{15b}$$

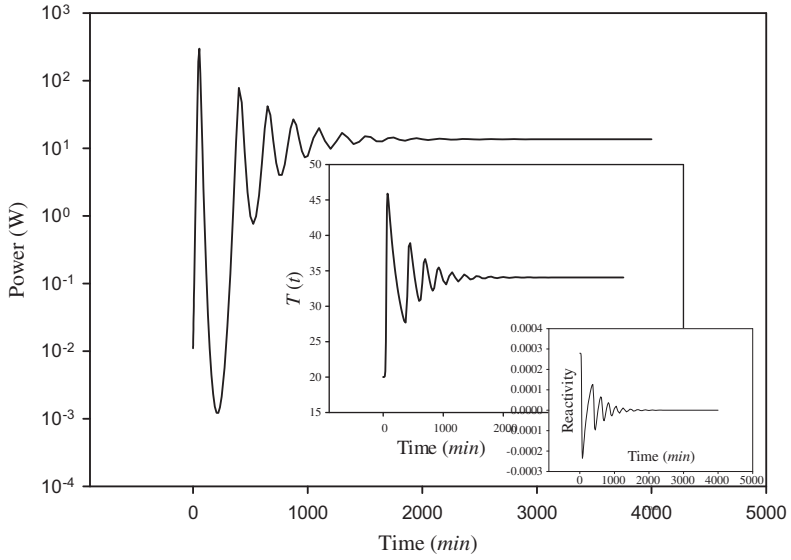

Fig. 5a. SKINATH application out to 4000 min.

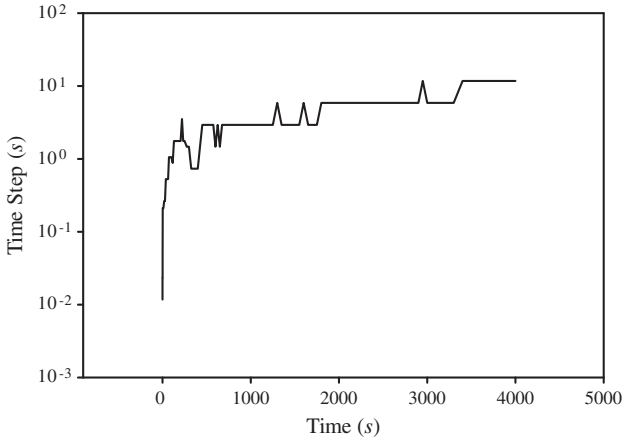

Fig. 5b. Minimum time step variation over 4000 min.

with

$$W(t) \equiv T(t) - T_c \tag{15c}$$

$W(t)$ is now added to the **y** vector of Eq. (3b) and the Jacobian matrix becomes

$$A\left(t,N(t),W(t)\right) \equiv \begin{bmatrix} \left(\rho\left(t,N(t)\right)-\beta\right)/\Lambda & \lambda_1 & \ldots & \lambda_m & 0 & 0 \\ \frac{\beta_1}{\Lambda} & -\lambda_1 & 0 & \ldots. & \ldots. & 0 \\ \ldots. & 0 & \ldots. & & & \ldots. \\ \frac{\beta_m}{\Lambda} & \ldots. & & -\lambda_m & & 0 \\ \frac{1}{C_p} & 0 & \ldots. & \ldots. & 0 & -u(t) \\ \frac{\rho_c}{C_p} & 0 & \ldots. & \ldots. & 0 & -\rho_c u(t) \end{bmatrix},$$

where

$$u(t) \equiv \frac{ahd^{0.75}}{C_p}\left[\frac{W(t)}{W(t)+T_c}\right]^{0.25}$$

Now the within-time-step iteration for the Jacobian will be on N and W. In addition, the inversion in Eq. (5) is performed by LU decomposition.

The SKINATH model is now applied to the thermal system of Table 6a with the system power, temperature and reactivity traces shown in Fig. 5a. The evolution is essentially identical to that of the SKINATH calculation, but here taken out to 4000 min to show the eventual return to criticality. The computational time[1] for a relative error of 10^{-5} is about 0.5*s* and for a relative error of 10^{-10} about 3.5 s as compared to 1.8*s* on an IBM 3033 platform for a 1000 min transient. Thus, we see a speed up of about 2 (over several decades) but for approximately 5 additional digits of accuracy. Fig. 5b gives the time step variation over the time evolution indicating the adaptive nature of the BEFD scheme. The ultimate verification is given in Table 6b, where we observe confirmation of the SKINATH code to nearly 4 figures (emboldened digits are in disagreement with PKE/BEFD). This confirms the conclusion of the conclusions made by the SKINATH authors concerning accuracy in 1984.

5. Conclusions

From the fundamental backward Euler difference scheme, a highly accurate algorithm, called PKE/BEFD, for the numerical solution of the reactor point kinetics equations has emerged. Such an algorithm has eluded practitioners in the quest for faster, cheaper, more accurate solutions to the PKEs, until now. The elegance of the algorithm is in its straightforward simplicity, "teachability" and extraordinary accuracy. For the first time, 7–9 place accurate benchmarks for the common cases found in the literature have been routinely established. If desired however, higher accuracy could be achieved simply by using FORTRAN quadruple precision (QP) rather than double precision (DP). QP would increase the computational time (conservatively) by a factor of 4, thus requiring about 4 min, rather than the 1 min required for all computations found above (except for the QP application). More accuracy, at the expense of computational time, could also be achieved if the BEFD algorithm were switched out for a higher order algorithm, such as a Heun or Runge-Kutta scheme.

Another significant feature of the PKE/BEFD algorithm is that it is fully time-step adaptive. Thus, it is no longer required to solve

[1] All computations performed on a VAIO 2.4 GHz dual core laptop.

the PKEs with a single time step; and we can get away from the "game" of perfecting the so-called "single time-step efficient" code and exchange "efficient" for "accurate" to focus on the meaningful issue.

The value of combining finite difference and convergence acceleration was demonstrated on several recently published methods and indicated the exaggerated declarations of accuracy that have been made. For those readers who doubt the accuracy of the PKE/BE algorithm, it should be remarked that all cases, but the last three for sinusoidal insertion and §4.2c, and those of the last section have been confirmed by an independent Taylor series algorithm (Ganapol et al., 2012) to *all* places quoted.

Finally, it should be emphasized, that the accuracy of the PKE/BEFD algorithm was achievable 40 years ago. While today's computational speeds enable the practicality of the algorithm, the underlying concepts were in place since 1971 (Izumi and Noda, 1971), but never came together until now.

References

Aboanber, A., Hamada, Y., 2002. PWS: An efficient code system for solving space-independent nuclear reactor dynamics. Ann. Nucl. Ener. 29, 2159–2172.

Aboanber, A.E., Hamada, Y.M., 2003. Power series solution (PWS) of nuclear reactor dynamics with newtonian temperature feedback. Ann. Nucl. Ener. 30, 1111–1122.

Aboanber, A.E., Nahla, A.A., 2002. Solution of the point kinetics equations in the presence of newtonian temperature feedback by padé approximations via the analytical inversion method. J. Phys. A: Math. Gen. 35, 3245–3263.

Dodds, H.L., Westfall, R.M., 1984. SKINATH – A Computer Program for Solving the Reactor Point Kinetics Equations with Simple Thermal-Hydraulic Feedback. ORNL/CSD/TM-210.

Ganapol, B. et al., 2012. The Solution of the Point Kinetics Equation: a Converged Accelerated Taylor Series (CATS), PHYSOR 2012, Knoxville, TN, USA, April 15–20, 2012, on CD-ROM. American Nuclear Society, LaGrange Park, IL.

Hindmarsh, A.C., 1980, LSODE and LSODI – Two New Initial. Value Ordinary Differential Equation Solvers. ACN-Signum Newsletter, Vsl. 15, No. 4.

Izumi, M., Noda, T., 1971. An implicit method for solving the lumped parameter reactor-kinetics equations by repeated extrapolation. Nucl. Sci. Eng. 41, 299–303.

Keepin, R.G., 1965. Physics of Nuclear Kinetics. Addison-Wesley, USA.

Kinard, M., Allen, E., 2004. Efficient numerical solution of point kinetics equations in nuclear dynamics. Ann. Nucl. Energy 31, 1039–1051.

Nahla, A.A., 2008. Generalization of the analytical exponential model to solve the point kinetics equations of Be- and D_2O-moderated reactors. Nucl. Eng. Des. 238, 2648–2653.

Nahla, A.A., 2010. Analytical solution to solve the point kinetics equations. Nucl. Eng. Des. 240, 1622–1629.

Nahla, A.A., 2011. An efficient technique for the point reactor kinetics equations with Newtonian temperature feedback effects. Ann. Nucl. Energy 38, 2810–2817.

da Nobrega, J.A.W., 1971. A new solution of the point kinetics equations. Nucl. Sci. Eng. 46, 366–375.

Petersen, C.Z., Dulla, S., Vilhena, M.T.M.B., Ravetto, P., 2011. An analytical solution of the point kinetics equations with time-variable reactivity by the decomposition method. Prog. Nucl. Energy 53, 1119–1125.

Stoer, J., Burlirsch, R., 1980. Introduction to Numerical Analysis. Springer-Verlag.

Vigil, J., 1967. Solution of the reactor kinetics equations by analytic continuation. Nucl. Sci. Eng. 29, 392–401.